

Programmed Pore Architectures in Modular Quaternary Metal–Organic Frameworks

Lujia Liu,[†] Kristina Konstas,[‡] Matthew R. Hill,[‡] and Shane G. Telfer^{*,†}

[†]MacDiarmid Institute for Advanced Materials and Nanotechnology, Institute of Fundamental Sciences, Massey University, Palmerston North 4442, New Zealand

[‡]CSIRO Materials Science and Engineering, Private Bag 33 Clayton South, Victoria 3169, Australia

S Supporting Information

ABSTRACT: To generate metal–organic frameworks (MOFs) that are complex and modular yet well ordered, we present a strategy employing a family of three topologically distinct linkers that codes for the assembly of a highly porous quaternary MOF. By introducing substituted analogues of the ligands, a set of eight isorecticular frameworks is delivered, with the MOF structure systematically varied while the topology is maintained. To combat randomness and disorder, the substitution patterns of the ligands are designed to be compatible with their crystallographic site symmetries. MOFs produced in this way feature “programmed pores”—multiple functional groups compartmentalized in a predetermined array within a periodic lattice—and are capable of complex functional behavior. In these examples unconventional CO₂ sorption trends, including capacity enhancements close to 100%, emerge from synergistic effects. Future PP-MOFs may be capable of enzyme-like heterogeneous catalysis and ultrasensitive adsorption.

To tackle the challenge of generating metal–organic framework (MOF) materials with sophisticated properties, inspiration may be drawn from enzymes where active site functionality emerges from the spatial arrangement of specific functional groups in a well-defined compartment.¹ In this spirit, we are pursuing MOFs with complex yet well-ordered and periodic pore architectures by copolymerizing sets of multiple topologically distinct ligands bearing different functional groups. Since combinations of linker backbones codes for a predetermined framework topology, and different linkers are located in predetermined positions in the crystalline lattice, *multiple functional groups are consequently located in predefined positions in the MOF pores*. This defines the first design principle for programming regular spatial arrays of multiple functional groups in MOF void spaces.

These materials, which we term programmed-pore MOFs (PP-MOFs), generate complexity without sacrificing homogeneity. They are distinct from MOFs constructed from an isostructural set of linkers² or that are simple derivatives of parent frameworks (e.g., UCMCM-1-NH₂³). Regularity and periodicity are achieved by high-fidelity sorting and arrangement of the different ligands during framework growth and careful matching of their substitution patterns to the space group symmetry to mitigate against both crystallographic and positional disorder.

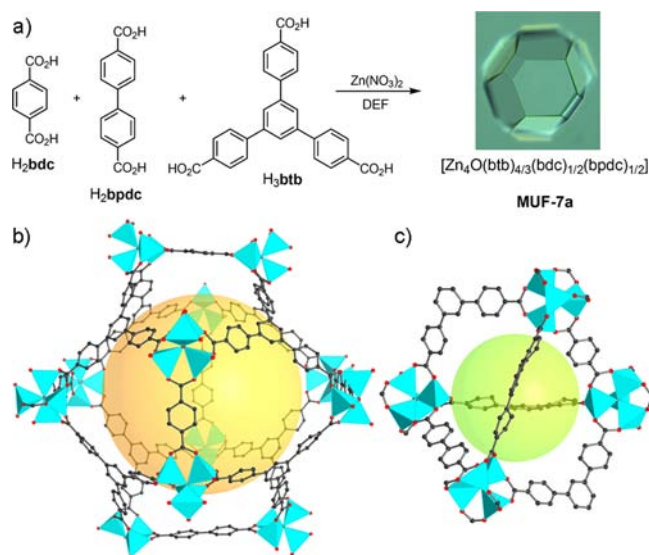


Figure 1. (a) Synthetic route to MUF-7a. (b) X-ray crystal structure of MUF-7a highlighting the large dodecahedral void. (c) Tetrahedral void delineated by one bdc, one bpdc, and four btb linkers.

To develop an experimental strategy toward the synthesis of PP-MOFs we required (i) a MOF composed of multiple topologically distinct ligands, (ii) functionalized analogues of this set of linkers that can be synthesized, and (iii) a framework topology that is conserved upon introduction of functionalized ligands. For proof-of-principle experiments we decided to pursue zinc(II) MOFs with polytopic aromatic carboxylate ligands to draw upon the known propensity of these frameworks to be highly open and porous.⁴ Although several known ternary MOFs (i.e., frameworks constructed from a set of two topologically distinct ligands) met our criteria,⁵ only two different functional groups would be introduced to the MOF pores. To introduce greater complexity we sought a MOF constructed from *three* topologically distinct ligands.

Combining Zn(NO₃)₂, H₃btb (btb = benzene-1,3,5-tribenzoate), H₂bdc (bdc = 1,4-benzenedicarboxylate), and H₂bpdc (bpdc = 4,4'-biphenyldicarboxylate) produces a MOF with a formula [Zn₄O(btbb)_{4/3}(bdc)_{1/2}(bpdc)_{1/2}] (MUF-7a, MUF = Massey University Framework) (Figure 1a). X-ray crystallog-

Received: September 29, 2013

Published: November 1, 2013

raphy shows that MUF-7a belongs to the cubic space group $I\bar{4}3d$ and comprises Zn_4O secondary building units (SBUs) that link the bdc, bpdc, and btb ligands into a periodic framework (Figures 1b and S3). To our knowledge, MUF-7 is the first quaternary member of the well-studied zinc(II) arylcarboxylate family of MOFs. Successful incorporation of the requisite three ligands into this MOF is achieved by cross-linking the four-connected nodes of a **pto** net,⁶ described by the btb ligand and four equatorial sites on the Zn_4O SBU, with two ditopic linkers of *different lengths* (Figure S3). The resulting framework is an **ith-d** net, which is isoreticular to $[Zn_4O(btb)_{4/3}(2,6\text{-naphthalenedicarboxylate})]$ (MOF-205/DUT-6).^{5c,7}

MUF-7a has a framework density of 0.387 g/cm³, and the void fraction of the material, calculated by the helium insertion method,⁸ is 0.89. The framework void spaces can be conceptualized as (i) a large dodecahedral cavity, highlighted by the orange sphere in Figure 1b, whose vertices are defined by the Zn_4O clusters and the centroids of the btb ligands and (ii) pseudotetrahedral void spaces that surround this dodecahedral cavity and connect to it via each of its 12 pentagonal windows (Figure S4). Three similar yet distinct tetrahedral void spaces are delineated by four btb ligands together with (a) pairs of bdc ligands, (b) pairs of bpdc ligands, and (c) a bdc/bpdc pair (Figure 1c). Allowing for the van der Waals radii of the framework atoms, the dodecahedral mesopore spans nearly 30 Å at its widest point and accommodates a sphere of 20 Å diameter (Figure 1b). The tetrahedral voids measure ~16 Å between the edges described by the concave btb ligands and 10 Å between the edges described by the bdc/bpdc ligand pairs. Apertures of ~9 × 12 Å define the free pore diameter of MUF-7a and connect the dodecahedral and tetrahedral voids into a contiguous pore system (Figure S3).

Although many competing structures can be produced from H_3btb , H_2bpdc , H_2bdc , and zinc(II), e.g., $[Zn_4O(btb)_2]$ (MOF-177),⁹ $[Zn_4O(bdc)_3]$ (MOF-5),¹⁰ $[Zn_4O(bpdc)_3]$ (IRMOF-9/10),¹¹ $[Zn_4O(btb)_{4/3}(bdc)]$ (UMCM-1),^{5a} and $[Zn_4O(bdc)_2(bpdc)]$ (SUMOF-4),¹² phase-pure MUF-7a was obtained by optimizing the ratio of precursors and the reaction conditions (see Supporting Information (SI) for details). As expected from the inherently different reaction rates of tritopic and ditopic ligands,¹³ adding the ligands in their stoichiometric ratios produced an abundance of MOF-177 crystals. To counteract this, an excess of ditopic ligands was employed, though we found that their ratio had to be biased toward bpdc to suppress crystallization of UMCM-1. To confirm the phase purity of MUF-7a we used PXRD, ¹H NMR spectroscopy on digested samples, and elemental analysis.

MUF-7a provided an ideal platform to develop our strategy for synthesizing PP-MOFs. Programmed variants of this framework require systematic replacement of one, two, or three of its linkers with substituted analogues. Maintaining perfect regularity and periodicity of the pores while the parent structure is elaborated in this way involves careful consideration of the symmetries and conformations of the ligands and their crystallographic site symmetries (Figure S2). For example, because the bdc ligand resides on a crystallographic 2-fold symmetry element that lies in the ligand plane perpendicular to its long axis, to preclude disorder by crystallographic symmetry this ligand should be functionalized with identical groups on its 2,3 positions or on its 2,3,5,6 positions. Coplanarity of the carboxyl groups and phenyl rings is much more likely in the former case than the latter, which informed the choice of naphthalene-1,4-dicarboxylate (ndc, Figure 2) as an analogue of bdc. Similarly, the bpdc ligand also

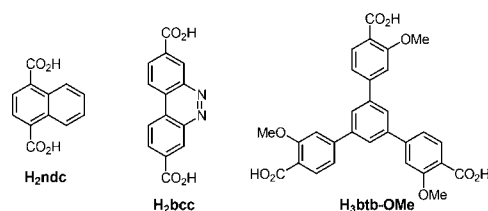


Figure 2. Substituted ligands designed to generate programmed-pore analogues of MUF-7a.

lies on a 2-fold crystallographic symmetry axis that relates the two phenyl rings. In this case, a 2,2' or 2,2',6,6' substitution pattern will prevent disorder by crystallographic symmetry. Also, a fully planar ligand conformation is geometrically disposed to generating a framework isoreticular to MUF-7a. Benzo[*c*]-cinnoline ligand bcc was selected with these considerations in mind (Figure 2). With respect to the btb component, 3-fold symmetry and ligand planarity should be retained. These criteria are met by the known methoxy-substituted ligand btb-OMe (Figure 2).^{3b}

Single-crystal X-ray diffraction (XRD) experiments showed that combinations of bdc/ndc, bpdc/bcc, and btb/btb-OMe yield a set of MOFs, MUF-7b-h, that adopt the $I\bar{4}3d$ space group and **ith-d** network topology of MUF-7a (Table 1). MUF-7 joins a select group of isoreticular frameworks that are tolerant to ligand substitution.^{11,14} Synthetic protocols for MUF-7b-h are broadly similar to that of MUF-7a, although, as noted for related tertiary MOFs,^{5a,13} reaction conditions must be carefully tuned to obtain phase-pure material in good yields. We observed that the yield and crystallinity of many of the frameworks could be improved by seeding techniques (see SI for details). Optical microscopy, powder XRD (Figure S5), and ¹H NMR on dissolved samples (SI) all indicate phase purity for these materials.

As intended, unfunctionalized ligands of MUF-7a are directly replaced in the MOF lattice by their substituted counterparts in MUF-7b-h (Figure 3). The ligand crystallographic site symmetries observed for MUF-7a are retained. Since the substitution patterns of ndc, bcc, and btb-OMe ligands were designed to be compatible with their site symmetries, no crystallographic disorder of the ligand substituents is evident. In addition, we closely analyzed the electron density maps generated from single-crystal XRD patterns of MUF-7b-h to determine whether the ligands display any noncrystallographic positional disorder (Figures S6–S15). From these maps this mode of disorder can be ruled out: ligand substituents are located exclusively on one side of the carboxyl-carboxyl axis (ndc and bcc) or of the centroid-carboxyl axes (btb-OMe). [The only apparent disorder involves minor rotational displacements of the naphthyl ring of ndc and the bridging phenyl rings of btb and btb-OMe, as detailed in the SI.]

These X-ray crystallographic results demonstrate that MUF-7a-h constitutes a set of PP-MOFs. The btb/bpdc/bdc ligand set reliably codes for a quaternary framework with predictable topology. The framework components are modular, and careful ligand design influences pore architectures in a predetermined and systematic way, introducing complexity but maintaining periodicity and circumventing randomness.

Thermogravimetric analysis demonstrates that MUF-7a-h retain ~50–70 wt% solvent upon exchange with CH_2Cl_2 (Figure S1), consistent with the large void spaces observed by X-ray crystallography. Upon careful activation, these MOFs are permanently porous. At 77 K, N_2 adsorption isotherms exhibit

Table 1. Summary of the Key Properties of MUF-7a and Programmed-Pore Analogues, MUF-7b-h

	MUF-7a	MUF-7b	MUF-7c	MUF-7d	MUF-7e	MUF-7f	MUF-7g	MUF-7h
linker set	bdc bpdcc btb	bdc bcc btb	ndc bpdcc btb	ndc bcc btb	bdc bpdcc btb-OMe	bdc bcc btb-OMe	ndc bpdcc btb-OMe	ndc bcc btb-OMe
unit cell length ^a	60.2324(11)	60.2289(7)	60.2326(6)	60.2136(6)	60.3052(11)	60.2594(6)	60.290(2)	60.2419(6)
space group	<i>I</i> 43 <i>d</i>	<i>I</i> 43 <i>d</i>	<i>I</i> 43 <i>d</i>	<i>I</i> 43 <i>d</i>	<i>I</i> 43 <i>d</i>	<i>I</i> 43 <i>d</i>	<i>I</i> 43 <i>d</i>	<i>I</i> 43 <i>d</i>
density ^b	0.387	0.392	0.396	0.401	0.429	0.435	0.438	0.444
surface area ^c	4140	4480	3910	3790	3910	3000	3820	4000
pore volume ^d	1.94	2.15	1.84	1.84	1.84	1.30	1.74	1.93
CO ₂ uptake ^e	30.3	32.3	31.5	30.5	46.4	37.5	52.7	58.8

^aIn Å. ^bIn g/cm³, determined from X-ray crystal structure. ^cIn m²/g, derived from N₂ sorption isotherm at 77 K using the BET method.¹⁵ ^dIn cm³/g, calculated from N₂ sorption isotherms at 77 K. ^eExcess sorption at 273 K and 1200 mbar, in cm³/g(STP).

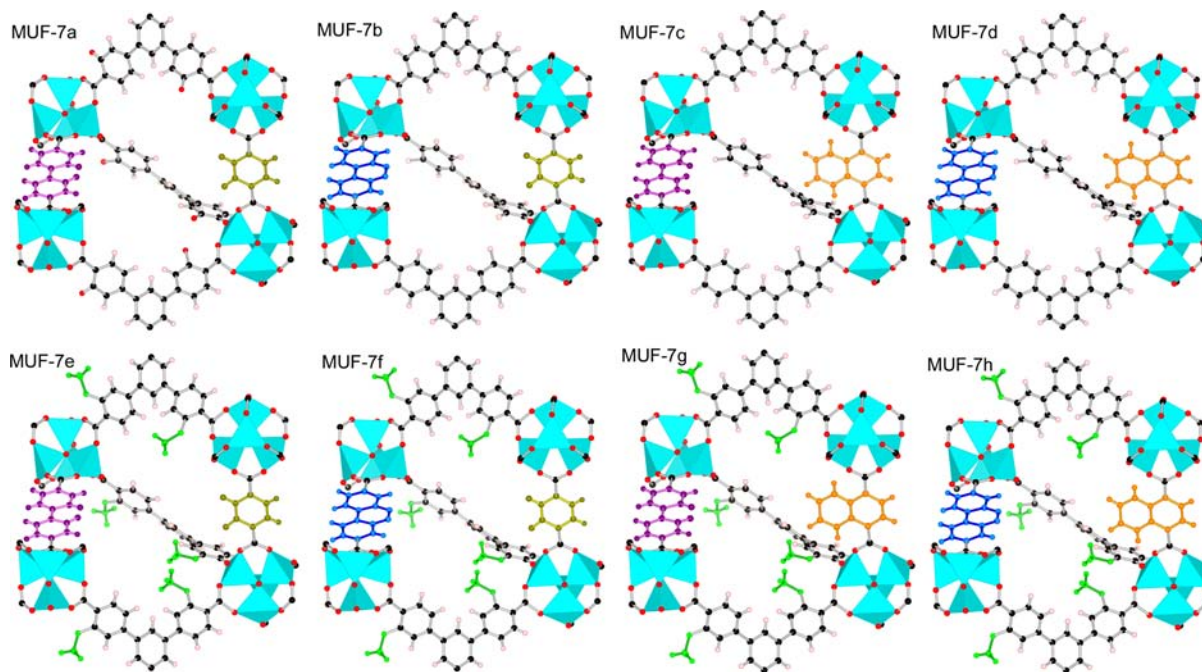


Figure 3. Systematic modulation of the three ligands of MUF-7a to produce MUF-7b-h. This delivers an isoreticular set of MOFs with programmed pores. The bpdcc ligand is highlighted in purple, bcc in blue, bdc in khaki, ndc in orange, and the methoxy groups of btb-OMe in green.

maximum N₂ uptake capacities between 800 and 1400 cm³(STP)/g (Figure S16). A step characteristic of mesoporous materials is observed at $P/P_0 \approx 0.05$. Analysis using the BET model¹⁵ (Figures S18–S25) indicates that these MOFs have high accessible surface areas and total pore volumes (Table 1), as anticipated from their crystal structures. MUF-7f exhibits slightly reduced values due to difficulties in fully activating this material. The measured surface area of MUF-7a (4140 m²/g) is close to its calculated¹⁶ geometric surface area (4181 m²/g).

Control over pore architectures afforded by the PP-MOF strategy induces significant changes in experimentally determined pore size distributions (Figure 4). Across the MUF-7a-h series, smaller and topographically more complex pores appear. Importantly, the overall pore volume is maintained since the large dodecahedral pore, with a width of ~ 19 Å, is largely unaffected by pore programming.

CO₂ adsorption isotherms illustrate the beneficial effects of programmed pore environments on functional MOF properties. Systematic modulation of the framework structure from MUF-7a to MUF-7h increases CO₂ adsorption capacity by 94% (Figure 5). For a set of materials that possess BET surface areas within 10% of one another upon full activation and that are devoid of strongly basic adsorption sites, this is a considerable gain, far in excess of the typical effects of ligand modulation.¹⁷ At 14–20 Å,

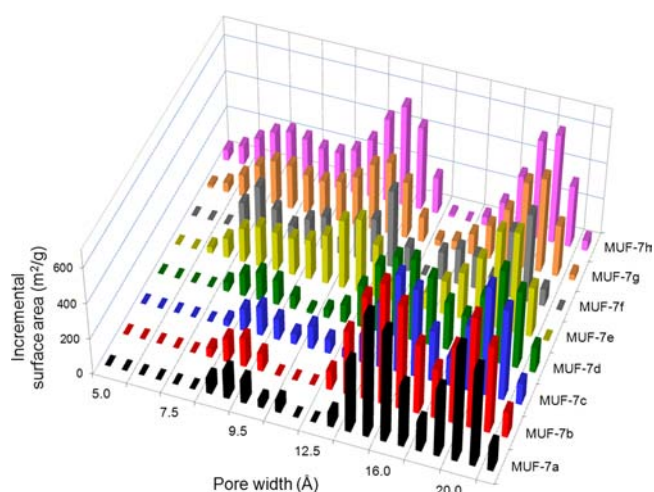


Figure 4. Pore size distribution plots for MUF-7a-h, calculated using a DFT method from N₂ isotherms measured at 77 K.

typical pore sizes in MUF-7a are larger than optimal for low-pressure CO₂ adsorption. However, increasing concentrations of smaller void spaces in MUF-7b-h (Figure 4) correlate with higher CO₂ adsorption capacities. In turn, this leads to enhancements in

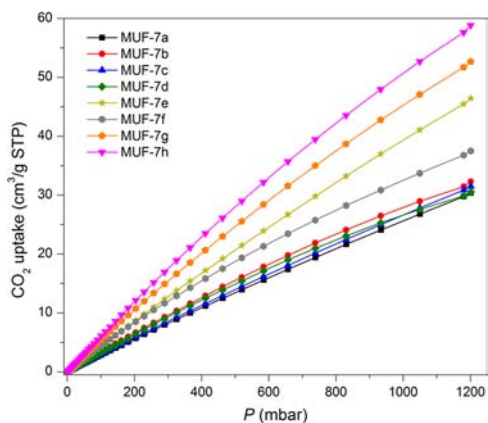


Figure 5. CO₂ adsorption isotherms measured for MUF-7a-h at 273 K.

isosteric heats of adsorption (Figure S17). Notably, ndc and bcc only have a pronounced impact on CO₂ sorption when btb-OMe, and not btb, is a coligand. This demonstrates that pore programming can induce synergistic effects among the ligands that elevate the properties of PP-MOFs beyond conventional frameworks.

Since the compartments of PP-MOFs can be programmed in advance, we envisage that materials more complex, diverse, and functional than the examples reported here can be achieved by (i) designing, synthesizing, and optimizing ligands bearing more exotic functional groups, (ii) deliberately targeting MOFs that conform to established design principles for high performance in specific applications,¹⁸ and (iii) producing frameworks built up from ligand sets comprising four or five members. Further, we expect it should be possible to couple PP-MOFs to our established thermolabile protecting group methodology¹⁹ to introduce substituents that may not otherwise be compatible with MOF synthesis conditions. Unprecedented properties will emerge from the ability to generate complex, programmed pore environments, e.g., enzyme-like heterogeneous catalysis and ultrasensitive guest sorption.

The challenges and opportunities associated with materials derived from multiple building blocks were identified in a recent review article: “the future of MOFs lies in the creation of materials whose constituents are many and are systematically varied.”⁴ The PP-MOF strategy presented here realizes this goal by copolymerizing multiple topologically distinct ligands to produce isorecticular sets of MOFs with systematically modulated structures. The randomness associated with previously reported complex MOFs is circumvented to produce periodic frameworks with pore architectures that can be predicted in advance. Enhanced properties emerge from PP-MOFs, and next-generation examples promise unique functionality.

■ ASSOCIATED CONTENT

📄 Supporting Information

Synthesis, characterization, and computational details, X-ray crystallography, and additional tables and figures. This material is available free of charge via the Internet at <http://pubs.acs.org>.

■ AUTHOR INFORMATION

Corresponding Author

s.telfer@massey.ac.nz

Notes

The authors declare no competing financial interest.

■ ACKNOWLEDGMENTS

We thank Prof. Jeffrey R. Long for valuable discussions and his research group for preliminary adsorption isotherms. Expert advice from Prof. Geoffrey B. Jameson, Prof. Randall Q. Snurr, and Pritha Ghosh is also acknowledged with gratitude. Parts of this work were funded by the Australian Science and Industry Endowment Fund.

■ REFERENCES

- (1) (a) Farrusseng, D.; Aguado, S.; Pinel, C. *Angew. Chem., Int. Ed.* **2009**, *48*, 752. (b) Lillerud, K. P.; Olsbye, U.; Tilset, M. *Top. Catal.* **2010**, *53*, 859.
- (2) (a) Kong, X.; Deng, H.; Yan, F.; Kim, J.; Swisher, J. A.; Smit, B.; Yaghi, O. M.; Reimer, J. A. *Science* **2013**, *341*, 882. (b) Deng, H.; Doonan, C. J.; Furukawa, H.; Ferreira, R. B.; Towne, J.; Knobler, C. B.; Wang, B.; Yaghi, O. M. *Science* **2010**, *327*, 846. (c) Bunck, D. N.; Dichtel, W. R. *Chem.—Eur. J.* **2013**, *19*, 818. (d) Park, T.-H.; Koh, K.; Wong-Foy, A. G.; Matzger, A. J. *Cryst. Growth Des.* **2011**, *11*, 2059. (e) Burrows, A. D.; Fisher, L. C.; Richardson, C.; Rigby, S. P. *Chem. Commun.* **2011**, *47*, 3380. (f) Kleist, W.; Jutz, F.; Maciejewski, M.; Baike, A. *Eur. J. Inorg. Chem.* **2009**, 3552. (g) Koh, K.; Wong-Foy, A. G.; Matzger, A. J. *Chem. Commun.* **2009**, 6162. (h) Burrows, A. D.; Frost, C.; Mahon, M. F.; Richardson, C. *Angew. Chem., Int. Ed.* **2008**, *47*, 8482.
- (3) (a) Wang, Z.; Tanabe, K. K.; Cohen, S. M. *Inorg. Chem.* **2009**, *48*, 296. (b) Dau, P. V.; Tanabe, K. K.; Cohen, S. M. *Chem. Commun.* **2012**, *448*, 9370.
- (4) Furukawa, H.; Cordova, K. E.; O’Keeffe, M.; Yaghi, O. M. *Science* **2013**, *341*, 974.
- (5) (a) Koh, K.; Wong-Foy, A. G.; Matzger, A. J. *Angew. Chem., Int. Ed.* **2008**, *47*, 677. (b) Koh, K.; Oosterhout, J. D. V.; Roy, S.; Wong-Foy, A. G.; Matzger, A. J. *Chem. Sci.* **2012**, *3*, 2429. (c) Furukawa, H.; Ko, N.; Go, Y. B.; Aratani, N.; Choi, S. B.; Choi, E.; Yazaydin, A. Ö.; Snurr, R. Q.; O’Keeffe, M.; Kim, J.; Yaghi, O. M. *Science* **2010**, *329*, 424.
- (6) Wells, A. F. *Structural Inorganic Chemistry*, 5th ed.; Oxford University Press: Oxford, U.K., 1984.
- (7) Klein, N.; Senkowska, I.; Gedrich, K.; Stoeck, U.; Henschel, A.; Mueller, U.; Kaskel, S. *Angew. Chem., Int. Ed.* **2009**, *49*, 9954.
- (8) Frost, H.; Düren, T.; Snurr, R. Q. *J. Phys. Chem. B* **2006**, *110*, 9565.
- (9) Chae, H. K.; Siberio-Perez, D. Y.; Kim, J.; Go, Y. B.; Eddaoudi, M.; Matzger, A. J.; O’Keeffe, M.; Yaghi, O. M. *Nature* **2004**, *427*, 523.
- (10) Li, H.; Eddaoudi, M.; O’Keeffe, M.; Yaghi, M. *Nature* **1999**, *402*, 276.
- (11) Eddaoudi, M.; Kim, J.; Rosi, N.; Vodak, D.; Wachter, J.; O’Keeffe, M.; Yaghi, O. M. *Science* **2002**, *295*, 469.
- (12) Yao, Q.; Su, J.; Cheung, O.; Liu, Q.; Hedin, N.; Zou, X. *J. Mater. Chem.* **2012**, *22*, 10345.
- (13) Koh, K.; Wong-Foy, A. G.; Matzger, A. J. *J. Am. Chem. Soc.* **2010**, *132*, 15005.
- (14) (a) Kim, M.; Boissonnault, J. A.; Allen, C. A.; Dau, P. V.; Cohen, S. M. *Dalton Trans.* **2012**, *41*, 6277. (b) Henke, S.; Schneemann, A.; Wütscher, A.; Fischer, R. A. *J. Am. Chem. Soc.* **2012**, *134*, 9464. (c) Garibay, S. J.; Cohen, S. M. *Chem. Commun.* **2010**, *46*, 7700. (d) Kandiah, M.; Nilsen, M. H.; Usseglio, S.; Jakobsen, S.; Olsbye, U.; Tilset, M.; Larabi, C.; Quadrelli, E. A.; Bonino, F.; Lillerud, K. P. *Chem. Mater.* **2010**, *22*, 6632. (e) Biswas, S.; Ahnfeldt, T.; Stock, N. *Inorg. Chem.* **2011**, *50*, 9518.
- (15) Walton, K. S.; Snurr, R. Q. *J. Am. Chem. Soc.* **2007**, *129*, 8552.
- (16) Dueren, T.; Millange, F.; Ferey, G.; Walton, K. S.; Snurr, R. Q. *J. Phys. Chem. C* **2007**, *111*, 15350.
- (17) Rowsell, J. L. C.; Yaghi, O. M. *J. Am. Chem. Soc.* **2006**, *128*, 1304.
- (18) Wilmer, C. E.; Leaf, M.; Lee, C.; Farha, O. K.; Hauser, B. G.; Hupp, J. T.; Snurr, R. Q. *Nat. Chem.* **2012**, *4*, 83.
- (19) (a) Sen Gupta, A.; Deshpande, R. K.; Liu, L.; Waterhouse, G. I. N.; Telfer, S. G. *CrystEngComm* **2012**, *14*, 5701. (b) Lun, D. J.; Waterhouse, G. I. N.; Telfer, S. G. *J. Am. Chem. Soc.* **2011**, *133*, 5806. (c) Deshpande, R. K.; Minnaar, J. L.; Telfer, S. G. *Angew. Chem., Int. Ed.* **2010**, *47*, 4598.